Supplemental data. Gebert et al. (2008). F-Actin Organization and Pollen Tube Tip Growth in *Arabidopsis* are Dependent on the Gametophyte–specific Armadillo Repeat Protein ARO1.

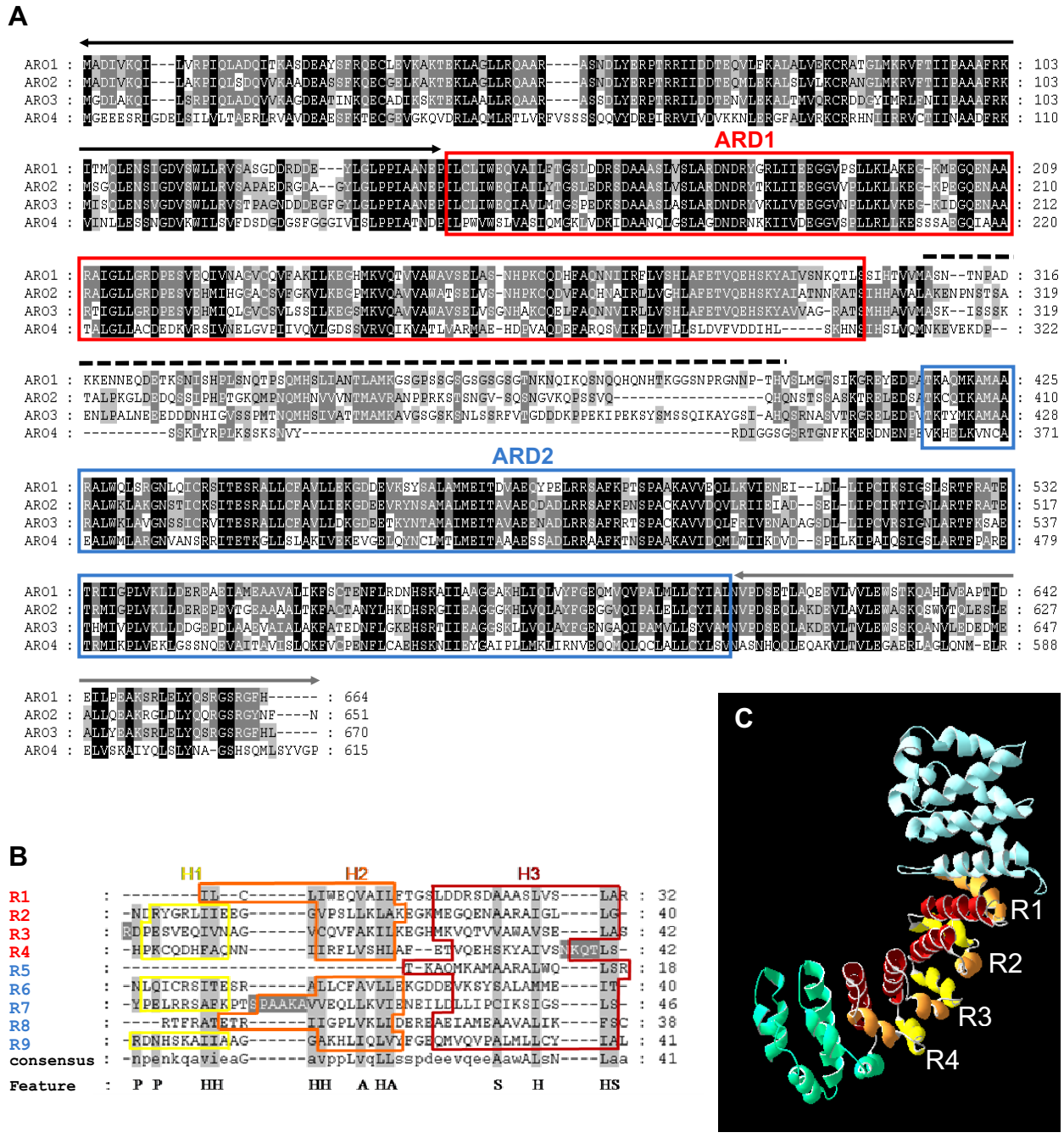

Supplemental Figure 1 online. *Arabidopsis* ARO proteins. (**A**) Primary structure of ARO1 to ARO4. The predicted protein sequences encoded by *ARO1*, *ARO2*, *ARO3*, and *ARO4* were aligned using M-Coffee and processed with GeneDoc. Letters in black blocks indicate identical amino acid residues/conserved substitutions, amino acid residues with more than 80% conservation are highlighted in dark grey, and those with more than 60% conservation are shown as light grey boxes. Two conserved ARM repeat domains (ARD1, ARD2) are located in the first and second half of each protein. ARD1 (boxed in red) and ARD2 (boxed in blue) are separated by a highly divergent "spacer" region of variable length (dashed line). A conserved domain of 143 to 153 amino acids is located at the N-terminus (black arrow) and a short stretch of 55 to 59 amino acids follows ARD2 at the C-terminus (grey arrow). (**B**) Sequence alignment of the nine putative ARM repeats (R1–R9) of ARO1 and the HMM ARM repeat consensus sequence (Pfam database; PF00514). R1 to R4 are located in ARD1, while R5 to R9 form ARD2. Putative helices H1 (yellow), H2 (orange) and H3 (red) of ARO1 were identified by PSIPRED secondary protein structure predictions. Note that R1, R5 and R8 represent incomplete ARM repeats. Conserved features of amino acids are indicated below the alignment. P, polar; H, hydrophobic; A, aliphatic; S, small. (**C**) Predicted 3D structure of ARO1 (amino acids 1–387), by homologous modeling with murine importin-α (*Mus musculus*; PDB Acc. 1ialA). ARO1 reveals a typical three-helical structure, forming a right handed superhelix of alpha-helices similar to importin-α. Although the N-terminal domain (blue) and the „spacer" (green) region do not contain recognized ARM repeats, their overall structure resembles the superhelical conformation of importin-α.

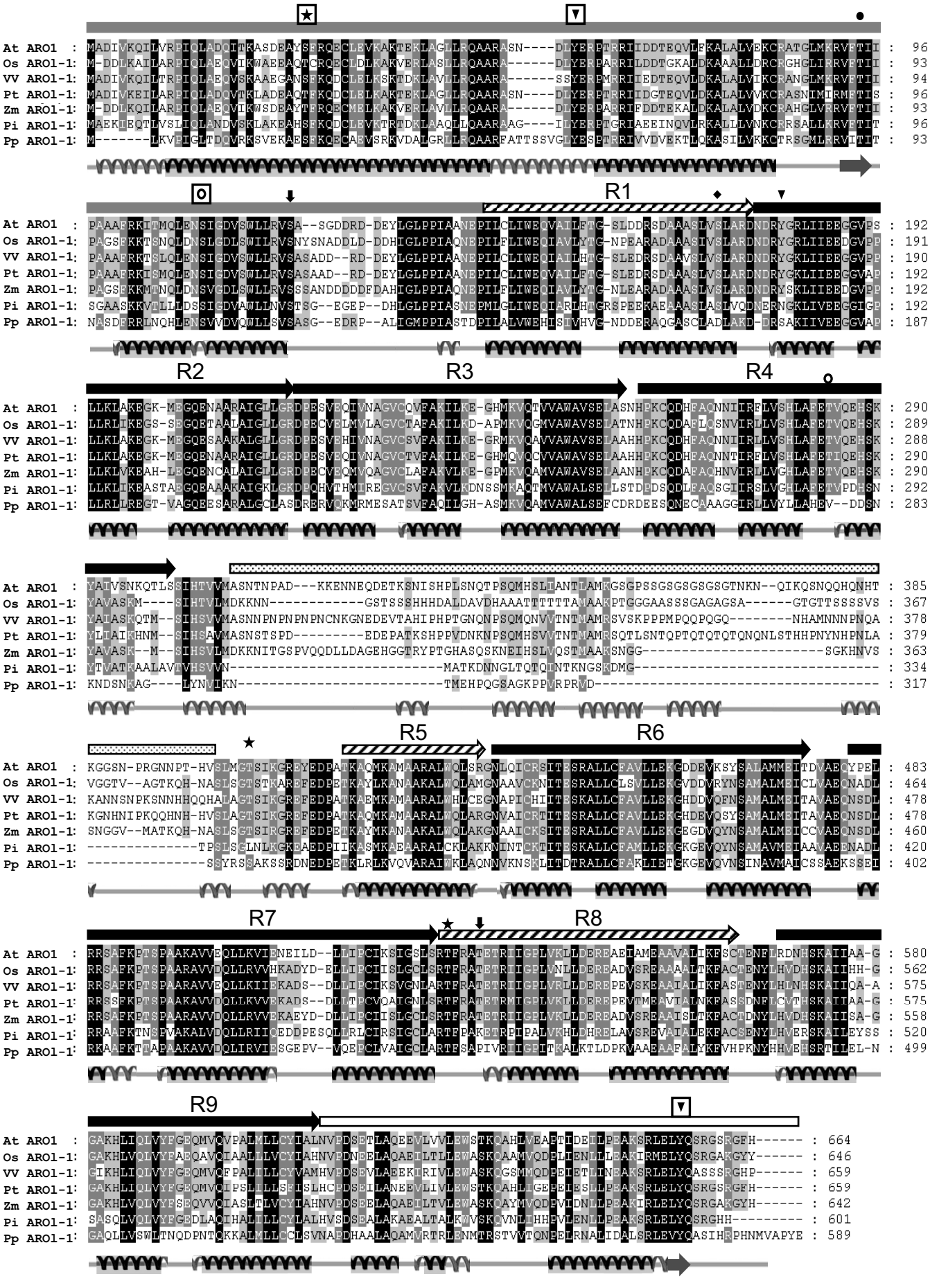
R1
R2
R3
R4
R5
R6
R7
R8
R9

Supplemental Figure 2 online. Conserved secondary structure and phosphorylation sites of ARO1-like proteins. The amino acid sequence of ARO1 was aligned with most similar ARO-like proteins from *Oryza sativa* (Os AROl-1), *Zea mays* (Zm AROl-1), *Vitis vinifera* (Vv AROl-1), *Populus trichocarpa* (Pt AROl-1), *Picea ssp.* (Pi AROl-1), and *Physcomitrella patens* (Pp AROl-1). Multiple sequence alignment and processing was performed using M-Coffee and GeneDoc. Letters in black blocks indicate identical amino acid residues/conserved substitutions, amino acid residues with more than 80% conservation are highlighted in dark grey, and those with more than 60% conservation are shown as light grey boxes. Secondary structure of ARO1-like proteins was predicted by PSIPRED. Twisted lines and broad arrows below alignment denote alpha-helices and beta-sheets, respectively. Conserved secondary structure elements found in all ARO1-like proteins are shaded. Phosphorylation sites were predicted by NetPhos, ELM, and PredictProtein. Protein kinase C (PKC) sites are marked by asterisks, vertical arrows indicate PKA sites, tyrosine phosphorylation sites are indicated by closed triangles, casein kinase (CK) II sites are marked by open circles, the CK I site is marked by a diamond. A possible 14-3-3 protein binding site is indicated by an closed circle. Boxed icons indicate phosphorylation sites conserved in all ARO1-like proteins, unboxed icons are sites conserved in angiosperm proteins, only. Positions of ARM repeats (R1 to R9) are depicted by arrows above the alignment. Black arrows: conserved ARM repeats; white arrows with diagonal stripes: imperfect ARM repeats. N- and C-terminal extensions are depicted as grey and open bars, respectively. The spacer region is labeled as a white bar with black dots.

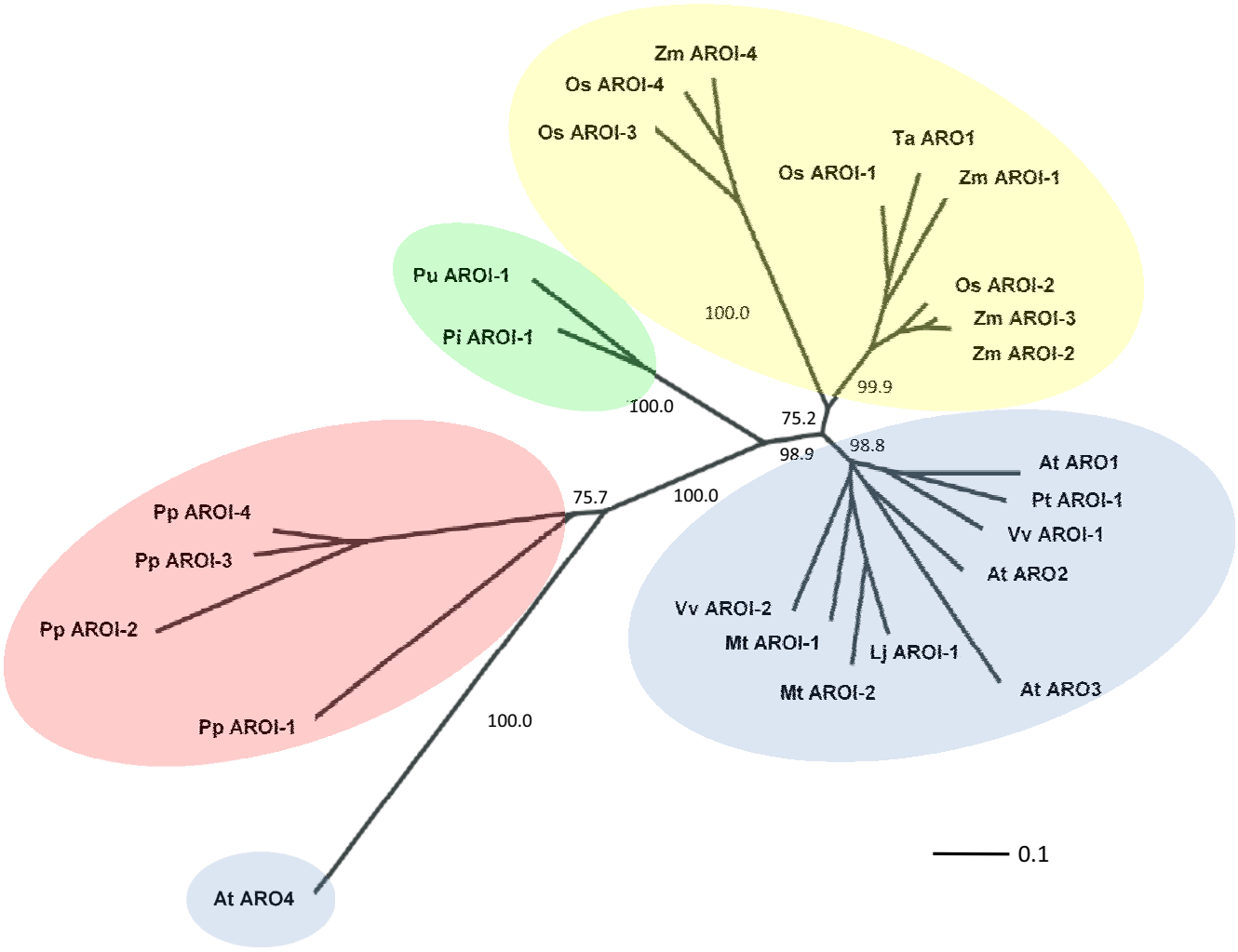

Supplemental Figure 3 online. Phylogenetic relationship of members of the *ARO* protein family. *Arabidopsis thaliana* ARO1 to -4, *Triticum aestivum* Ta ARO1 and identified putative ARO-like proteins of *Lotus japonicus* (Lj AROl-1), *Medicago truncatula* (Mt AROl-1; Mt AROl-2), *Oryza sativa* (Os AROl-1 to -4), *Vitis vinivera* (Vv AROl-1; Vv AROl-2), *Picea spp.* (Pi AROl-1), *Pinus spp.* (Pu AROl-1), *Populus trichocarpa* (Pt AROl-1), *Physcomitrella patens* (Pp AROl-1 to -4), and *Zea mays* (Zm AROl-1 to -4) were aligned using M-Coffee. A maximum likelihood distance matrix was calculated with SplitsTree. The clade formed by AROs from dicotyledonous plants is colored in blue, the monocotyledonous clade is highlighted in yellow, gymnosperm AROs are highlighted in green, and the clade of moss AROs is colored in red. Please note that Pi AROl-1 represents the predicted CDS of a tentative contig of assembled ESTs, and that Ta ARO1, Pp AROl-4 and Pu AROl-1 represent partial protein sequences. Distances of proteins are displayed as numbers of nucleotide substitutions per site. Scale bar: 0.1 nucleotide substitution per site. Sequences used to generate the phylogeny are presented in Supplemental Dataset 1 online.

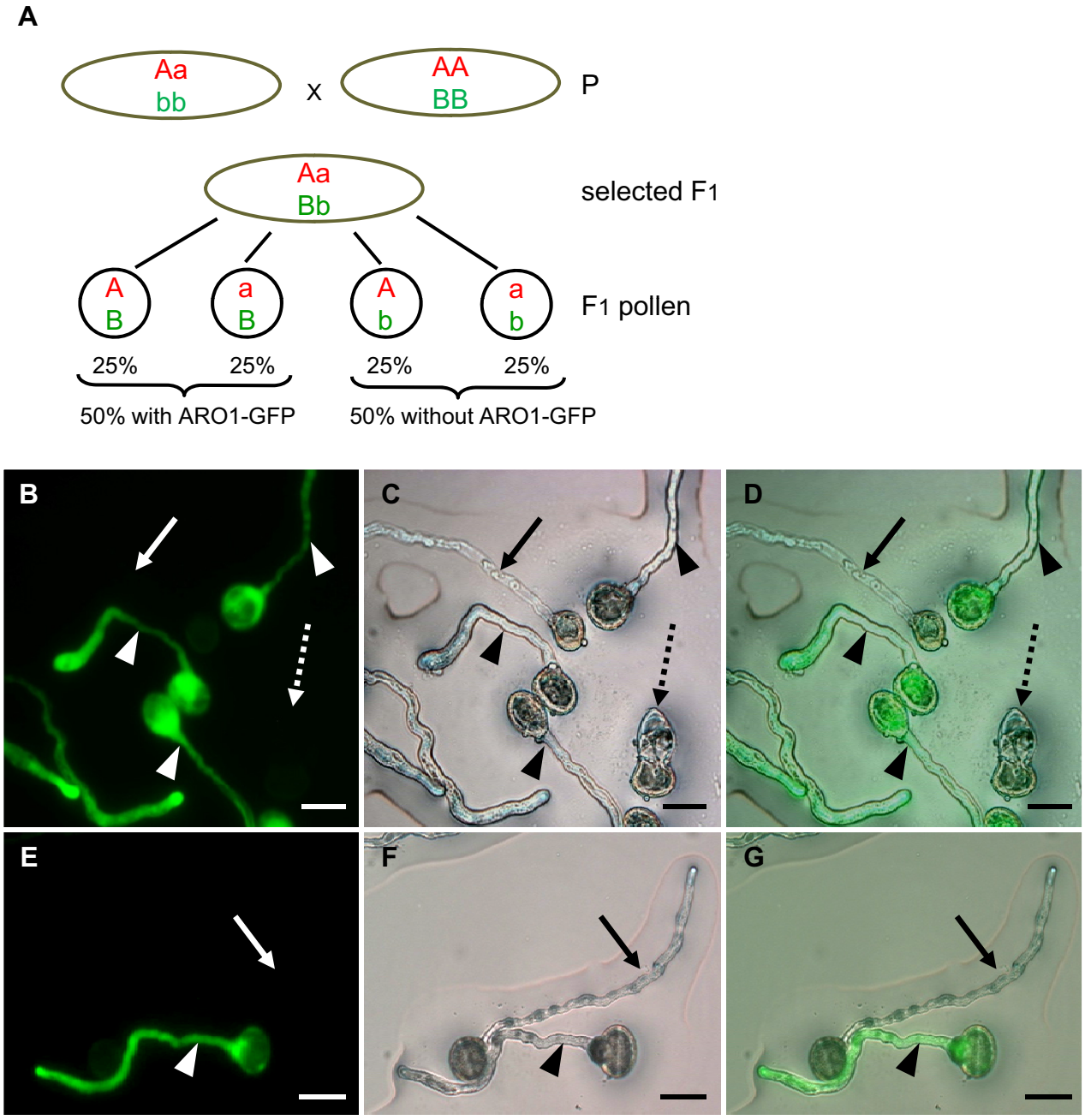

Supplemental Figure 4 online. Complementation of the *aro1-3* phenotype by ARO1-GFP. Homozygous plants expressing ARO1-GFP under control of the *ARO1* promoter (*AtARO1*$_{pro}$*:AtARO1-GFP*) were used for pollination of heterozygous *aro1-3/+* plants. (**A**) Scheme of the transmission of the ARO1/*aro1-3* (Aa) and the *ARO1-GFP* (Bb) allele. Heterozygous *aro1-3/+* plants (Aabb) were crossed with plants homozygous for ARO1-GFP (AABB). Amongst the progeny, only *aro1-3/+* plants were selected for *in vitro* pollen germination tests (F_1; AaBb). Possible allele combinations in the male gametophytes of these plants are indicated. 50% of all pollen should express ARO1-GFP, and half of these pollen should carry the *aro1-3* allele. (**B**) to (**D**) Approximately 50% of the germinated pollen tubes expressed ARO1-GFP. All GFP fluorescent pollen tubes looked phenotypically normal (arrowheads), while 25% of the non-fluorescent pollen tubes revealed the *aro1-3* phenotype (dashed arrow). (**E**) to (**G**) In the progeny of wild-type plants crossed with homozygous *ARO1*$_{pro}$*:AtARO1-GFP* plants, 50% of all pollen tubes showed GFP fluorescence (arrowhead). ARO1-GFP expression did not cause obvious alterations in pollen tube morphology, compared to wild type (arrow). (**B**), (**E**) Fluorescence images; (**C**), (**F**), bright field images; (**D**), (**G**), merged pictures. Scale bars: 20 µm.

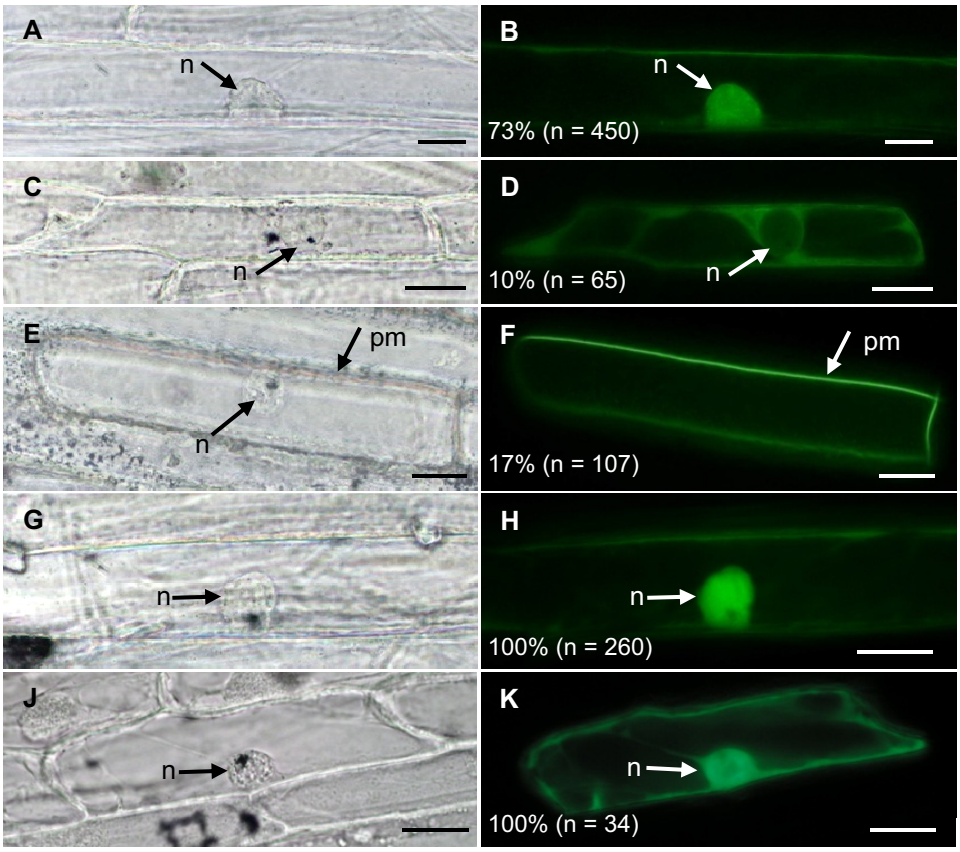

Supplemental Figure 5 online. ARO1-GFP distribution in spring onion epidermal cells. Bright field and epifluorescence images of spring onion epidermal cells transiently expressing ARO1-GFP (**A** to **F**) and ARO2-GFP (**G**, **H**) fusion proteins under control of the maize *UBI* promoter. *UBI_{pro}:GFP* (**J**, **K**) was used as a control. 24 hours after biolistic transformation, expressing cells were scored for their subcellular localization of fluorescence. Observed localization patterns are expressed as a percentage of the total number of transformed cells. Numbers in parenthesis indicate absolute numbers of transformed cells showing the respective expression pattern. (n) nucleus, (pm) plasma membrane. Scale bars: 40 µm.

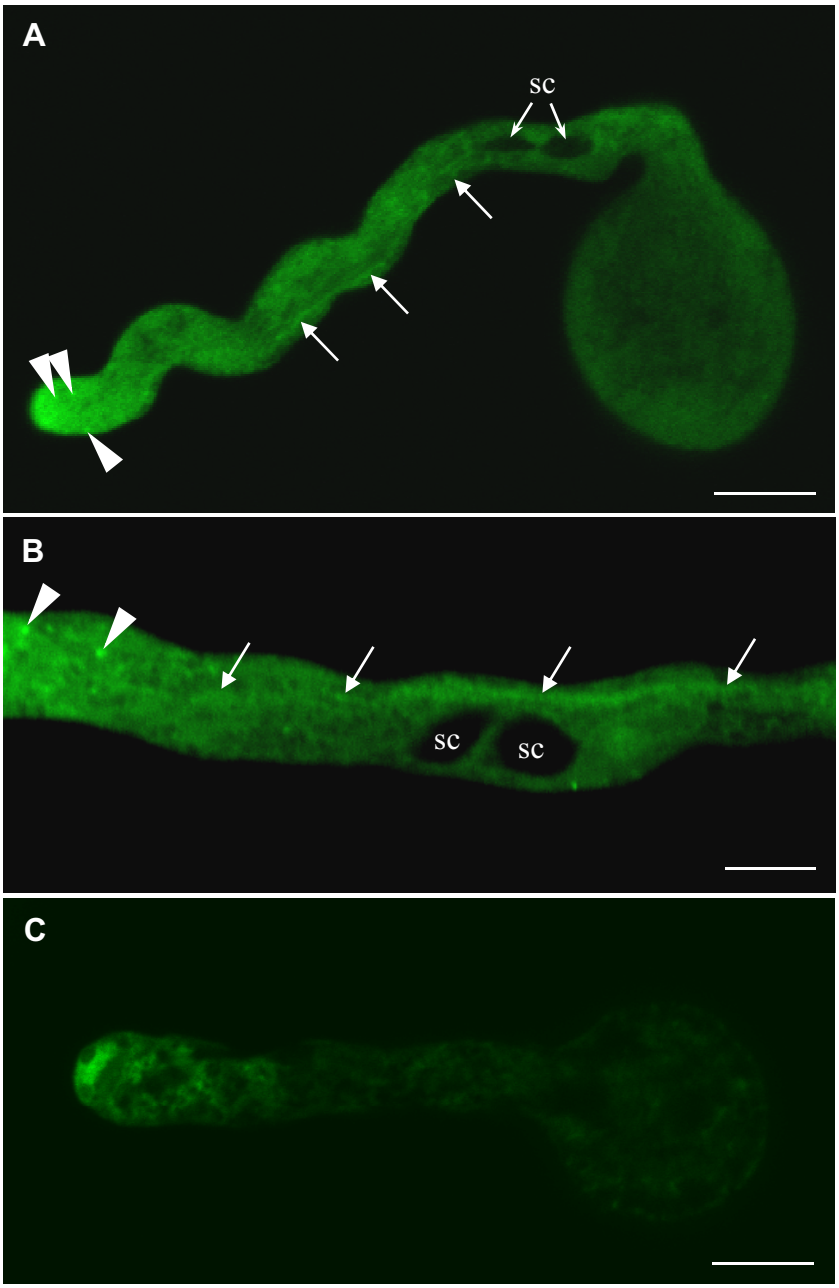

Supplemental Figure 6 online. CLSM live imaging of ARO1-GFP before and after LatB treatment. (**A**) and (**B**) Single medial optical sections of *in vitro* germinated pollen tubes expressing *ARO1p:AtARO1-GFP*. The fusion protein reveals some filament-like fluorescence in the shank of pollen tubes. Longer filament-like fluorescent signals align with the tube axis, especially in the central portion of the pollen tube (arrows), while fluorescent spots appear to be enriched mainly in the apical region (arrowheads); tube tip in (B) orients towards the left side; the tube tip in (A) is not in focus. (**C**) Single medial optical sections of an *in vitro* germinated *ARO1p:AtARO1-GFP* expressing pollen tube treated with LatB. The GFP signal appeared weaker and more cloudy and dispersed than that of untreated transgenic pollen tubes. No filament-like fluorescent structures are visible in the shank. Optical sections in (**A**) 0.61 µm, (**B**) 0.48 µm, (**C**) 0.40 µm. sc; sperm cells; Scale bars (**A**) and (**C**) 10 µm, (**B**) 5 µm.

A

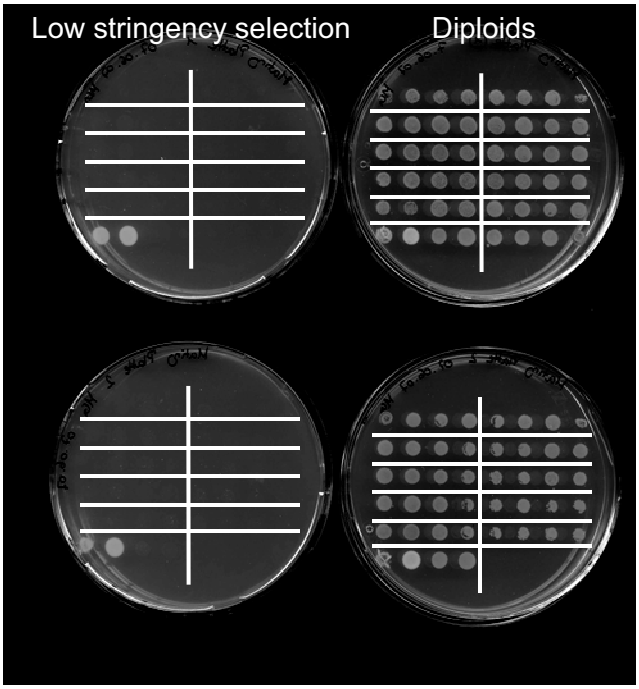

B

four replicas	four replicas
A1-BD x A1-AD	A1-AD x A1-BD
A1-BD x Act3-AD	A1-AD x Act3-BD
A1-BD x Act4-AD	A1-AD x Act4-BD
A1-BD x Act7-AD	A1-AD x Act7-BD
A1-BD x GFP-AD 1	A1-AD x GFP-BD
2 replicas +/ two replicas -	A1-AD x 0-BD

four replicas	four replicas
A1-BD x lam-BD	GFP-AD x GFP-BD
GFP-BD x GFP-AD	GFP-AD x Act3-BD
GFP-BD x Act3-AD	GFP-AD x Act4-BD
GFP-BD x Act4-AD	GFP-AD x Act7-BD
GFP-BD x Act7-AD	GFP-AD x 0-BD
2 replicas +/ two replicas -	

Supplemental Figure 7 online. ARO1 does not interact with different actin monomers of *Arabidopsis*, as tested by a yeast two-hybrid assay. Interactions were tested between ARO1 and ACT3, ACT4, ACT7, or GFP, respectively. In addition, auto-activation of each ARO1 and GFP was tested. (**A**) Low stringency selection of mated diploid yeast cells. Plates on the right hand side represent replica plates of diploid yeast cells plated on SD/-Leu/-Trp. On the left hand side, clones from diploids were tested for protein interactions. Only the positive control grew on low stringency SD/-Leu/-Trp/-His plates, indicating that none of the fusion proteins investigated in this study interact with each other or with themselves. (**B**) Scheme of spotted yeast clones shown in (**A**). After mating, four representative clones from diploids were spotted onto selective media as indicated. A1, ARO1; AD, activation domain; BD, binding domain; GFP, green fluorescent protein; lam, human lamin C (negative control); p53, murine p53; RecT, large T-antigen; 0-BD, empty pGBKT7 vector; +, positive control (RecT-AD x p53-BD); -, negative control (RecT-AD x lam-BD).

Supplemental Table 1 online. Gametophytic transmission efficiency of the *aro1-3* allele.

Crosses[a] (female x male)	Progeny		
	aro1-3/+	+/+	TE (%)
+/+ x *aro1-3/+*	0	38	0 (n = 38)
aro1-3/+ x +/+	36	35	50.70 (n = 71)
aro1-3/+ x *aro1-3/+*	42	51	45.16 (n = 93)

[a] Reciprocal crosses of wt (+/+) and heterozygous *aro1-3/+* plants were carried out by hand-pollination of emasculated wt pistils with *aro1-3/+* pollen, and *vice versa*. As a control, *aro1-3/+* plants were self-pollinated. Progeny were analyzed for T-DNA integration. Values represent absolute numbers of *aro1-3/+* and wt progeny plants as well as the transmission efficiency (TE) of the *aro1-3* mutant allele through the male and female gametophytes, respectively. Numbers in parentheses indicate total number of analyzed plants (n). TE of the *aro1-3* mutant allele in self-pollinated *aro1-3/+* plants is slightly below the TE of *aro1-3/+* plants pollinated with wt pollen.

Supplemental Methods

Bioinformatics

The cDNA sequence and the corresponding ORF of wheat clone EC-123 (EU662204) were used as queries to run BLASTX 2.2.17 and TBLASTN 2.2.17 searches in the nucleotide collection (nr/nt) database at NCBI (http://www.ncbi.nlm.nih.gov). At ARO1 (NP_195220) and Os AROl-1 (BAD09952) protein sequences were used as queries to run TBLASTN searches in the Plant Genome Database (http://www.plantgdb.org; *Zmbac* database), and in the *Populus* genome release 1.1 (http://genome.jgi-psf.org/Poptr1_1/Poptr1_1.home.html). Tentative Consensus sequences (TCs) of assembled ESTs of pine and spruce were identified by performing TBLASTN searches in the corresponding TGI databases (http://compbio.dcfi.harvard.edu/tgi/). ORFs of corresponding genomic sequences or ESTs were identified and translated into proteins using Clone Manager 6 (©Scientific & Educational Software) and EditSeq 4.05 (Lasergene, ©1989-2000 DNAStar Inc). Translated protein sequences were analysed and processed using the programs M-Coffee (Moretti et al., 2007) and GeneDoc 2.7.000 (Nicholas and Nicholas, 1997). Phylogenetic relationships of ARO-like proteins were calculated after importing a multiple sequence alignment obtained from the M-Coffee web server into SplitsTree4 (Huson & Bryant, 2006). A maximum likelihood distance matrix was determined using a JTT model (Jones et al., 1992) and neighbour-joining method (Saitou and Nei, 1987). Statistic significance of single branches was verified with bootstrapping (1000 replicates). The Conserved Domain search service (http://www.ncbi.nlm.nih.gov/Structure/ cdd/wrpsb.cgi), the Pfam 22.0 and HMMPfam 2.3.2. databases (http://pfam.sanger.ac.uk/; http://hmmpfam.ddbj.nig.ac.jp/top-e.html), and PSIPRED v2.5 secondary protein structure predictions (http://bioinf.cs.ucl.ac.uk/psipred/psiform.html) were used to identify ARM repeats. Putative phosphorylation sites were predicted by ELM (http://elm.eu.org/), NetPhos2.0 (http://www.cbs.dtu.dk/services/NetPhos/) and PredictProtein (http://www.predictprotein.org/). Homologous modeling of 3-D structures was made using the DeepView/ Swiss-Pdb viewer 3.7 (http://www.expasy.org/spdbv).

Primer sequence*s*

Sequences of primers used for the experiments mentioned in the manuscript were as follows:

Primers used for PCR, RT-PCR, and sequencing

LP1-1	5′-CAAGTTAGACAAGCATTGGAACC-3′
Rp1-1	5′-TTTCACAATATCCGCCATGAG-3′
LP1-2	5′-CAGAGACACGTAGGAGCCAAG-3′
RP1-2	5′-AAGCTGGTGTCCTTGACTGTG-3′
LP1-3	5′-TACCACAAGCCGTGCCAACTT-3′
RP1-3	5′-CGATCATCGAGAGAGCCTGTGA-3′
LBa1	5′-TGGTTCACGTAGTGGGCCATCG-3′
Act3fw	5′-GATTTGGCATCACACTTTCTACAATG-3′
Act3rev	5′-GTTCCACCACTGAGCACAATG-3′
ARO1fw	5′-TGAGTATTTAGGTCTCCCTC-3′
ARO1rev	5′-GCCGCGTTTTCTTGACCTTCC-3′
ARO2fw	5′-AGCGCATCCAAGACTCG-3′
ARO2rev	5′-AAGCCCATTCCAACACTG-3′
ARO3fw	5′-AATGGCGAGTAAAATCAGTAGTG-3′
ARO3rev	5′-GGTATCTTTTCCGGGGGTTTA-3′
ARO4fw	5′-TCGGCTTGCTCAAATGCTTAGAACACT-3
ARO4rev	5′-GATTTGCCCCTCCGCCGATGAA-3′
eIF4fw	5′-CGGCGATGTTCTTGGGAGTG-3′
eIF4rev	5′-CCGGTTAGGTGCATGAGGTTTG-3′

Primers used for cloning

ARO1pfw	5′-TAAAGagatctAAGCTGGTGTC-3′ (*BglII* site included)
ARO1prev	5′-CGCCATGagatctAACAATCAA-3′(*BglII* site included)
PAro1F	5′-CTCTcggccgcgATCTAAGCTGGTGT-3′ (*NotI* site included)
PAro1R	5′-CCCCactagtAACAATCAAGAAACTC-3′ (*SpeI* site included)

ARO1GFPfw 5′-TTGTcctaggTCATGGCGGATATTGTGAAACAG-3′ (*AvrII* site included)

ARO1GFPrev 5′-CGTCcctaggCAATGAAATCCTCTTGACCCTC-3′ (*AvrII* site included)

ARO2GFPfw 5′-CTGAcctaggCGATGGCAGACATCGTCAAG-3′ (*AvrII* site included)

ARO2GFPrev 5′-AATAcctaggCAATTGAAATTGTAACCCCTTGATCC-3′ (*AvrII* site included)

Primers used for cloning yeast vectors

Y2H/Aro1-NcoI 5′-TTCccatggCGGATATTGTGAAACAG-3′

Y2H/Aro1-SmaI 5′-cccgggCATATATCAATGAAATCCTCTTGA-3′

Y2H/Act3-NcoI 5′-TCCTCGAGAGTAGAccatggCTGAT-3′

Y2H/Act3-SmaI 5′-GGCTTCcccgggAGCAGACTTAACT-3′

Y2H/Act4-NcoI 5′-CCAGATTGAAccatggCGGACGGTG-3′

Y2H/Act4-SmaI 5′-GAcccgggATTAGAAGCATTTCCTATGC-3′

Y2H/Act7-NcoI 5′-AAGTGAAccatggCCGATGGTGAGG-3′

Y2H/Act7-SmaI 5′-cccgggTAGAAGCATTTCCTGTGAAC-3′

Y2H/GFP-NcoI 5′-ccatggGCAAGGGCGAGGAACTGTT-3′

Y2H/GFP-SmaI 5′-GATCcccgggTCACTTGTAGAGTTCATCC-3′

Generation of constructs for expression of GFP fusion proteins

Constructs *UBI_{pro}:ARO1-GFP* and *UBI_{pro}:ARO2-GFP* were generated by cloning eGFP (Pang et al., 1996) to the C-terminus of both ARO1 and ARO2. The ORFs of *ARO1* and *ARO2* were amplified from genomic DNA using Advantage Genomic Polymerase Mix (Clontech) and the primer pairs ARO1GFPfw/ARO1GFPrev and ARO2GFPfw/ARO2GFPrev, respectively. After ligation into pCR®-Blunt II-TOPO® (Invitrogen), *ARO1* and *ARO2* were each cut out by *AvrII*, thereby removing the stop codons, and ligated into pLNU-GFP (DNA Cloning Service), likewise digested with *AvrII* but dephosphorylated. For cloning the binary vector *$ARO1_{pro}$:ARO1-GFP*, the *ARO1* promoter was amplified from *$ARO1_{pro}$:GUS* using the primer pair PAro1F/PAro1R. By digesting the plasmid *UBI_{pro}:ARO1-GFP* with *NotI*/*SpeI*, the UBI promoter was removed and replaced by ligating the *NotI*/*SpeI* digested *ARO1* promoter fragment. The cloned cassette of *$ARO1_{pro}$:ARO1-GFP* was then transferred into the binary

vector 95P-Nos (DNA Cloning Service) via *Sfi* digest and ligation. *Agrobacterium tumefaciens* strain GV3101 (pMP90RK) was used for transformation of *Arabidopsis* Col-0 by "floral dip", according to Clough & Bent (1998). Three days after germination, Kanamycin resistant plants were selected according to Xiang et al. (1999).

Complementation and reciprocal crosses

For reciprocal crosses, we used the heterozygous insertion line *aro1-3/+* as egg donor and wt plants as sperm donor, and *vice versa*. For complementation tests homozygous $ARO1_{pro}$*:ARO1-GFP* pollen was used to fertilize heterozygous *aro1-3/+* plants. Closed flower buds of flowers at stage 12 (according to Smyth et al., 1990) were emasculated and pollinated 48 hours later by hand using freshly dehiscent anthers. Pollen from at least two different anthers was used to pollinate each pistil. Progenies of reciprocal crosses were analyzed for T-DNA integration as described.

Transient transformation

For transient expression studies, each of the plasmids UBI_{pro}*:ARO1-GFP*, UBI_{pro}*:ARO2-GFP*, or *pLNU-GFP*, were used. Biolistic transformation of epidermal spring onion cell layers was performed as described previously (Dresselhaus et al., 2006) but using 5–10 µg of plasmid and 50 µl aliquots of a 60 mg/ml gold suspension (0.4-1.2 µm, Heraeus) for the preparation of plasmid-coated gold particles. Cells were bombarded with 7-10 µl aliquots of plasmid-coated gold particles, using the particle delivery system-1000/He (Bio-Rad).

Yeast two-hybrid interaction assay

Cloning of candidate genes

The direct interaction yeast two-hybrid assay was performed using the Matchmaker^{TM} GAL4 Two-Hybrid System 3 (Clontech) according the manufacturers guidelines. *ARO1* and candidate genes *Actin3* (*Act3,* At3g53750), *Actin4* (*Act4,* At5g59370), *Actin7* (*Act7,* At5g09810) were amplified from cDNA generated from leaves (*Act3*; *Act7*) or pollen (*ARO1*; *Act4*) of *Arabidopsis*, while *eGFP* was amplified from transgenic pollen of an *ARO1p:ARO1-GFP* plant. Open reading frames were amplified from 1 µl of corresponding cDNA using the TripleMaster PCR system (Eppendorf), 10x high fidelity buffer plus Mg^{2+}, 5% DMSO and

1M betaine. Primers used for amplification were Y2H/ARO1-NcoI and Y2H/ARO1-SmaI (*ARO1*), Y2H/Act3-NcoI and Y2H/Act3-SmaI (*Act3*), Y2H/Act4-NcoI and Y2H/Act4-SmaI (*Act4*), Y2H/Act7-NcoI and Y2H/Act7-SmaI (*Act7*), and Y2H/GFP-NcoI and Y2H/GFP-SmaI (*GFP*), introducing *in frame* restriction sites both at the 5´- and the 3´-end of each of the coding sequences. After restriction digest with *NcoI* and *SmaI*, the amplification products were ligated into vectors pGBKT7 and pGADT7, respectively. Cloned constructs were verified by sequencing and transformed into yeast strains AH109 and Y187, following the manufacturer's protocol. Expression of recombinant fusion proteins was verified by immunoblotting of yeast protein extracts according the manufacturer's guidelines, using polyclonal anti-c-Myc antibodies.

Mating and interaction test

Direct interaction assay of recombinant fusion proteins was carried out by mating the yeast strains, as specified in the manufacturer's protocol. Diploid cells were picked from four independent colonies of each mating combination using a 100 µl filter pipette tip. Picked colonies were re-suspended in 30 µl ddH_2O in a 96 well microtiter plate. The cell suspensions were plated onto selective media SD/-Leu/-Trp and SD/-Leu/-Trp/-His, respectively, using a replica plate with 48 prongs. After three days of growth at 30°C, plates were evaluated.

Supplemental References

Clough, S.J., and Bent, A.F. (1998). Floral dip: a simplified method for *Agrobacterium*-mediated transformation of *Arabidopsis thaliana*. Plant J. **16**: 735-743.

Dresselhaus, T., Srilunchang, K.-o., Leljak-Levanić, D., Schreiber, D. N., and Garg P. (2006). The fertilization induced DNA replication factor MCM6 of maize shuttles between cytoplasm and nucleus, and is essential for plant growth and development. Plant Physiol. **140**: 512-527.

Huson, D.H., and Bryant, D. (2006). Application of phylogenetic networks in evolutionary studies. Mol. Biol. Evol. **23**: 254-267.

Jones, D.T., Taylor, W.R., and Thornton, J.M. (1992). The rapid generation of mutation data matrices from protein sequences. Comput. Appl. Biosci. **8**: 275-282.

Moretti, S., Armougom, F., Wallace, I.M., Higgins, D.G., Jongeneel, C.V., and Notredame, C. (2007). The M-Coffee web server: a meta-method for computing multiple sequence alignments by combining alternative alignment methods. Nucleic Acids Res. **35**: 645-648.

Nicholas, K.B., Nicholas H.B. Jr., and Deerfield, D.W. II. (1997). GeneDoc: analysis and visualization of genetic variation. Embnew. News **4**: 14.

Pang, S.Z., DeBoer, D.L., Wan, Y., Ye, G., Layton, J.G., Neher, M.K., Armstrong, C.L., Fry, J.E., Hinchee, M.A., and Fromm M.E. (1996). An improved green fluorescent protein gene as a vital marker in plants. Plant Physiol. **112**: 893-900.

Saitou, N., and Nei, M. (1987). The neighbor-joining method: A new method for reconstructing phylogenetic trees. Mol. Biol. Evol. **4**: 406-425.

Xiang, C., Han, P., and Oliver, D.J. (1999). *In solium* selection for *Arabidopsis* transformants resistant to kanamycin. Plant Mol. Biol. Rep. **17**: 59-65.